Video Article

Lung MicroRNA Profiling Across the Estrous Cycle in Ozone-exposed Mice

Nathalie Fuentes[1], Patricia Silveyra[1,2]

[1]Pulmonary, Immunology and Physiology Laboratory, Department of Pediatrics, Pennsylvania State University College of Medicine

[2]Department of Biochemistry and Molecular Biology, Pennsylvania State University College of Medicine

Correspondence to: Patricia Silveyra at pzs13@psu.edu

URL: https://www.jove.com/video/58664
DOI: doi:10.3791/58664

Keywords: Air pollution, lung miRNome, bronchoalveolar lavage, lung inflammation, sex hormones, PCR arrays, estrous cycle, vaginal smear

Date Published: 12/19/2018

Citation: Fuentes, N., Silveyra, P. Lung MicroRNA Profiling Across the Estrous Cycle in Ozone-exposed Mice. *J. Vis. Exp.* (), e58664, doi:10.3791/58664 (2018).

Abstract

MicroRNA (miRNA) profiling has become of interest to researchers working in various research areas of biology and medicine. Current studies show a promising future of using miRNAs in the diagnosis and care of lung diseases. Here, we define a protocol for miRNA profiling to measure the relative abundance of a group of miRNAs predicted to regulate inflammatory genes in the lung tissue from of an ozone-induced airway inflammation mouse model. Because it has been shown that circulating sex hormone levels can affect the regulation of lung innate immunity in females, the purpose of this method is to describe an inflammatory miRNA profiling protocol in female mice, taking into consideration the estrous cycle stage of each animal at the time of ozone exposure. We also address applicable bioinformatics approaches to miRNA discovery and target identification methods using *limma*, an R/Bioconductor software, and functional analysis software to understand the biological context and pathways associated with differential miRNA expression.

Video Link

The video component of this article can be found at https://www.jove.com/video/58664/

Introduction

microRNAs (miRNAs) are short (19 to 25 nucleotides), naturally occurring, non-coding RNA molecules.Sequences of miRNAs are evolutionary conserved across species, suggesting the importance of miRNAs in regulating physiological functions[1]. microRNA expression profiling has been proven to be helpful for identifying miRNAs that are important in the regulation of a variety of processes, including the immune response, cell differentiation, developmental processes, and apoptosis[2]. More recently, miRNAs have been recognized for their potential use in disease diagnostics and therapeutics. For researchers studying mechanisms of gene regulation, measuring miRNA expression can enlighten systems-level models of regulatory processes, especially when miRNA information is merged with mRNA profiling and other genome-scale data[3]. On the other hand, miRNAs have also been shown to be more stable than mRNAs in a range of specimen types and are also measurable with greater sensitivity than proteins[4]. This has led to considerable interest in the development of miRNAs as biomarkers for diverse molecular diagnostic applications, including lung diseases.

In the lung, miRNAs play important roles in developmental processes and the maintenance of homeostasis. Moreover, their abnormal expression has been associated with the development and progression of various pulmonary diseases[5]. Inflammatory lung disease induced by air pollution has demonstrated greater severity and poorer prognosis in females, indicating that hormones and the estrous cycle can regulate lung innate immunity and miRNA expression in response to environmental challenges[6]. In this protocol, we use ozone exposure, which is a major component of air pollution, to induce a form of lung inflammation in female mice that occurs in the absence of adaptive immunity. By using ozone, we are inducing the development of airway hyperresponsiveness that is associated with airway epithelial cell damage and an increase in neutrophils and inflammatory mediators in proximal airways[7]. Currently, there are not well-described protocols to characterize and analyze miRNAs across the estrous cycle in ozone-exposed mice.

Below, we describe a simple method to identify estrous cycle stages and miRNA expression in lung tissue of female mice exposed to ozone. We also address effective bioinformatics approaches to miRNA discovery and target identification, with an emphasis on computational biology. We analyze the microarray data using *limma*, an R/Bioconductor software that provides an integrated solution for analyzing data from gene expression experiments[8]. Analysis of PCR array data from *limma* has an advantage in terms of power over t-test based procedures when using small number of arrays/samples to compare expression. To comprehend the biological context of miRNA expression results, we then used the functional analysis software. In order to understand the mechanisms regulating transcriptional changes and to predict likely outcomes, the software combines miRNA-expression datasets and knowledge from the literature[9]. This is an advantage when compared with software that just look for statistical enrichment in overlapping to sets of miRNAs.

Protocol

All methods described here have been approved by the Institutional Animal Care and Use Committee (IACUC) of Penn State University.

1. Assessment of the Estrous Cycle Stage

1. Properly restrain a female C57BL/6 mouse (8–9 weeks old) using the one-handed mouse restraint technique described in Machholz et al.[10].
2. Fill the sterile plastic pipette with 10 µL of ultra-pure water.
3. Introduce the tip of plastic pipette into the vagina.
4. Gently flush the liquid 4–5 times to collect the sample.
5. Place the final flush containing vaginal fluid on a glass slide.
6. Observe the unstained vaginal flush under a light microscope with a 20x objective.
   NOTE: Animals that do not show regular cycles due to pseudopregnancy or other causes need to be excluded from the experiment. It is recommended to perform daily vaginal secretions for at least three consecutive cycles to confirm cyclicity.

2. Exposure to Ozone

1. Place a maximum of 4 mice in two 1.2 L glass containers with wire mesh lids, and water ad libitum.
2. Put one glass container in the ozone chamber and the other in the filtered air exposure chamber.
3. Adjust the ozone concentration to 2 ppm and monitor ozone levels regularly.
   NOTE: The ozone apparatus delivers a regulated airflow (>30 air changes/h) with controlled temperature (25 °C) and relative humidity (50%). The system generates ozone by an electrical discharge ozonizer, which is monitored and controlled by an ultraviolet ozone analyzer and mass flow controllers, as described previously[11].
4. Remove glass containers after 3 h of ozone/filtered air exposure. Return animals to cage with bedding, food, and water ad libitum.

3. Lung Collection

1. 4 h after exposure, anesthetize animals with an intraperitoneal injection of a ketamine/xylazine cocktail (90 mg/kg ketamine, 10 mg/kg xylazine).
   NOTE: To confirm a proper level of anesthesia, check the mouse for a pedal reflex (firm toe pinch) and adjust the anesthetic as needed.
2. Dampen the mouse skin with 70% ethanol.
3. Make a 2 cm midline incision using an operating scissor and surgical tweezers to expose the vena cava.
4. Sacrifice mice by transection of the vena cava and aorta. If needed, insert a 21 G gauge needle into the vena cava above the renal veins to collect blood prior to exsanguination. Alternatively, collect blood via heart puncture following standard protocols.
5. Use a surgical scissor to cut open the abdominal cavity and remove skin/upper muscle, moving upwards toward the ribs.
6. Use a surgical scissor to puncture the diaphragm.
   NOTE: Lungs will collapse away from the diaphragm.
7. Cut away the ribcage using a surgical scissor to expose the heart and lungs.
8. Using forceps, take a 1.5 mL RNase-free microcentrifuge tube and submerge it in liquid nitrogen to fill the tube.
   NOTE: Use goggles and protective gloves to handle liquid nitrogen.
9. Remove the lungs, place them into the RNase-free microcentrifuge 1.5 mL tubes filled with liquid nitrogen to snap-freeze the tissue, and wait a few seconds until the liquid evaporates.
10. Close the tube lid and store the tissue at -80 °C until use.

4. RNA Preparation

1. Pulverize whole lungs using a stainless-steel tissue pulverizer.
   NOTE: The tissue pulverizer needs to be placed in liquid nitrogen prior to use. Clean the pulverizer after each use with RNAse solution.
2. Split the pulverized lungs and place into two 1.5 mL tubes (half lung each).
3. Add 500 µL of guanidinium thiocyanate per sample tube and mix. Homogenize each sample using 18 G, 21 G, and 23 G needles, respectively.
   NOTE: Samples can be spiked with 5.6 x 10^8 copies of a small RNA spike-in control (from a different species) before proceeding with the extraction.
4. Add 500 µL of ethanol to each sample and vortex for 15 s.
5. Load the mixture in a spin column in a collection tube and centrifuge at 12,000 x *g* for 1 min. Discard the flow-through.
6. **For DNase I treatment (in-column);**
   1. Add 400 µL of RNA Wash Buffer and centrifuge at 12,000 x *g* for 1 min.
   2. In an RNase-free tube, add 5 µL of DNase I and 75 µL of 1x DNA digestion buffer and mix. Add the mix directly to the column matrix.
   3. Incubate at room temperature for 15 min.
7. Add 400 µL of RNA prewash solution to the column and centrifuge at 12,000 x *g* for 1 min. Discard the flow-through and repeat this step.
8. Add 700 µL of RNA wash buffer to the column and centrifuge at 12,000 x *g* for 1 min. Discard the flow-through.
9. Centrifuge at 12,000 x *g* for 2 min to remove remaining buffer. Transfer the column into an RNase-free tube.
10. To elute RNA, add 35 µL of DNase/RNase-free water directly to the column matrix and centrifuge at 12,000 x *g* for 1.5 min.
11. Measure total RNA concentration (260 nm) and purity using a spectrophotometer. Follow instructions to perform RNA quantification in a 1.5 µL sample aliquot. Blank the instrument with DNase/RNase-free water used for elution.

NOTE: A 260/280 ratio of ~2.0 is generally accepted as "pure" for RNA. Typical RNA concentration usually ranges between 750 and 2,500 ng/µL.

12. Store at -80 °C.

5. miRNA Profiling

1. **To retro-transcribe small RNAs, use 200 ng of total RNA.**
    1. Prepare the reverse-transcription reaction mix on ice (total volume per reaction is 20 µL). For each reaction, add 4 µL of 5x buffer, 2 µL of 10x nucleotides mix, 2 µL of reverse transcriptase, and 2 µL of RNase-free water. Mix all the components and aliquot in 600 µL RNAse-free plastic tubes (10 µL of mix per reaction).
    NOTE: The reverse-transcription master mix contains all components required for first-strand cDNA synthesis except template RNA.
    NOTE: Calculate excess volume (10%) when preparing the master mix.
    2. Add the template RNA (200 ng in 10 µL) to each tube containing reverse-transcription master mix. Mix, centrifuge for 15 s at 1,000 x *g*, and store them on ice until placing in thermocycler or dry block.
    3. Incubate for 60 min at 37 °C.
    4. Incubate for 5 min at 95 °C and place the tubes on ice.
    5. Dilute the cDNA by adding 200 µL of RNase-free water to each 20 µL reverse-transcription reaction.

2. **Perform real-time PCR using the Mouse Inflammatory Response and Autoimmunity miRNA PCR Array.**
    1. Prepare a reaction mix (total volume 1100 µL): For each reaction, add 550 µL of 2x PCR master mix, 110 µL of 10x universal primer mix, 340 µL of RNase-free water, and 340 µL of template cDNA (diluted reaction from step 5.1.5).
    2. Add 10 µL of reaction mix to each well of the pre-loaded miRNA PCR Array using a multichannel pipettor.
    3. Seal the miRNA PCR Array plate with optical adhesive film.
    4. Centrifuge the plate for 1 min at 1,000 x *g* at room temperature to remove bubbles.
    5. Program the real-time cycler, PCR initial activation step for 15 min at 95 °C, 3-step cycling containing denaturation for 15 s at 94 °C, annealing for 30 s at 55 °C, and extension for 30 s at 70 °C for 40 cycles number.
    NOTE: Follow manufacturer's cycling conditions instructions to set up the real-time cycler. Perform the dissociation curve step built into the real-time cycler software.
    6. Perform data analysis.

6. Data Analysis

1. Extract Ct values from the real time PCR software for each sample into an analysis software.
NOTE: A Ct value of 34 is considered as cutoff. If samples contain spike-in control (e.g., cel-mir-39), normalize Ct values to the spike in control for each sample. Threshold values may need to be manually set. Baseline values are automatically set.
2. Normalize Ct values to the average Ct of six miRNA housekeeping controls: SNORD61, SNORD68, SNORD72, SNORD95, SNORD96A, RNU6-2, using the following equation:
ΔCt = (Ct_Target − Ct_housekeeping)
3. For fold change calculations, calculate ΔΔCt values using a specific sample as the control, using the relative expression equation[12]:
miRNA relative expression:
$2^{-\Delta\Delta}$*Ct, where -* $\Delta\Delta$*Ct = -[*Δ*Ct test -* Δ*Ct control]*
NOTE: A fold change of 200 is considered as cutoff.
4. Export fold change expression values to perform statistical analysis on R using the *limma* package in Bioconductor[8].
5. Correct for multiple comparisons using the Benjamini-Hochberg method[13].
NOTE: A copy of the R script is available at: http://psilveyra.github.io/silveyralab/. Datasets and analyzed data are also available at the Gene Expression Omnibus under number GSE111667, https://www.ncbi.nlm.nih.gov/geo/query/acc.cgi?acc=GSE111667.

7. Data Analysis: Functional Analysis Software

1. Arrange the dataset. Include miRNAs with their respective expression log ratios and p-values. See **Table 1** for specific dataset formatting.
2. Open functional analysis software (version 01-10).
3. Upload the dataset using the following format: File format: "Flexible Format", Contains Column Header: "Yes", Select Identifier type: "miRBase (mature)", Array platform used for experiments: Choose the array platform.
NOTE: Accepted files formats are .txt (tab delimited text files), .xls (excel files), and .diff (cuffdiff files).
4. Select "Infer Observations" and verify that the experimental group labeling is correct.
5. Go to "Dataset Summary" to revise the total amount of mapped and unmapped miRNAs.
6. **Click on the "new" button at the top left of program. Select "New MicroRNA Target Filter" and upload a microRNA dataset.**
    1. Set Source to: TarBase, Ingenuity Experts Findings, miRecords.
    2. Set Confidence to: Experimentally observed or high (predicted).
    3. Select "Add Columns" to include a variety of biological information about the targets such as species, diseases, tissues, pathways and more.
    4. To focus on targets that have changed expression in the experiment, select "Add/ replace mRNA dataset". Use "Expression Pairing" to locate microRNAs with the same or different expression levels.
    NOTE: The filter analysis will provide microRNA names and symbols, mRNA targets, the source that describes the target relationship, and the confidence level of the predicted relationship (**Figure 2**).

7. Click "Add to My Pathway" to send the filtered dataset to a pathway canvas and explore more biological relationships.

8. Use Path Designer to create a publication-quality model of microRNA effects.
9. **An alternate option is to create a core analysis.**
    1. For core analysis type, select “Expression Analysis”.
    2. For measurement type, select “Expr Log Ratio”.
    3. Analysis Filter Summary: consider only molecules and/or relationships where: (species = mouse) AND (confidence = experimentally observed) AND (data sources = “Ingenuity Expert Findings”, “Ingenuity ExpertAssist Findings”, “miRecords”, “TarBase”, OR “TargetScan Human”).
    4. Select a cutoff of p-value = 0.05.
    5. Run the analysis.
    NOTE: The report will include: canonical pathways, upstream regulators analysis, diseases and functions, regulator effects, networks, molecules and more.

Representative Results

The different cell types observed in smears are used to identify the mouse estrous cycle stage (**Figure 1**). These are identified by cell morphology. During proestrus, cells are almost exclusively clusters of round-shaped, well-formed nucleated epithelial cells (**Figure 1A**). When the mouse is in the estrus stage, cells are cornified squamous epithelial cells, present in densely packed clusters (**Figure 1B**). During metestrus, cornified epithelial cells and polymorphonuclear leukocytes are seen (**Figure 1C**). In diestrus, leukocytes (small cells) are generally more prevalent (**Figure 1D**).

We extracted RNA from four mouse lungs following the protocol previously described. The nucleic acid concentrations (ng/ µL) ranged between 1197.9 and 2178.1 with an average of 1583.1 ± 215 (**Table 1**). The average A260/A280 ratio fluctuated from 2.010 to 2.020 with an average of 2.016 ± 0.002. On the other hand, the observed A260/A230 ratios oscillated between 2.139 and 2.223 with an average of 2.179 ± 0.018.

Table 2 shows differential expression results obtained with *limma* on R. We calculated top differentially expressed miRNAs between mice exposed to ozone or filtered air in proestrus (using the command toptable)[14]. The first column gives the value of the log2-fold fold change in miRNA expression between ozone and filtered air exposed animals. The column t represents the moderate t-statistic calculated for each miRNA in the comparison. The columns p.value and adj.p.value represent associated p-values for each comparison before and after multiple testing adjustment, respectively. Adjustment for multiple comparisons was done with the Benjamini and Hochberg's method to control the false discovery rate[15]. Column B represents the log-odds that the miRNA is differentially expressed[8].

We performed the miRNA target filter and core analysis that includes the enrichment pathway analysis. After uploading a list of 14 miRNAswith the significant expression log ratio and p-value, all of them were mapped by the miRNA target filter (**Table 3**). The results were filtered and sorted to get to certain pathways, in this case the "Cellular Immune Response". The core analysis provided information about canonical pathways, diseases and function, regulators, and networks (**Table 4**). The functional analysis software produced a network analysis that shows the relationship between the miRNAs of interest and other molecules (**Figure 3**).

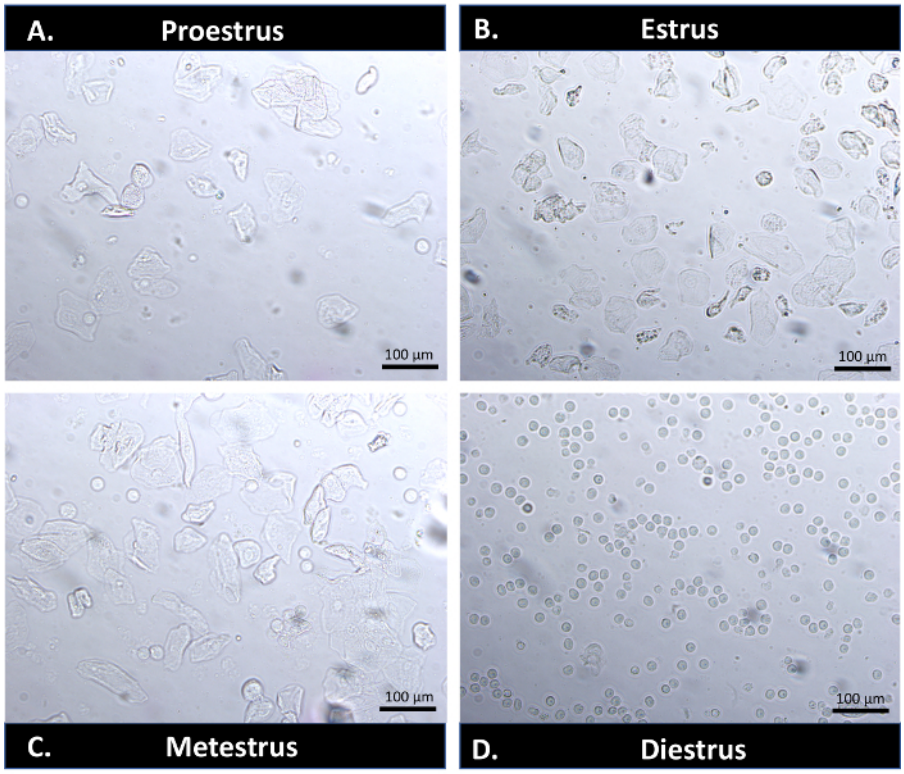

Figure 1: Identification of estrous cycle stages. (**A**) Proestrus (predominantly nucleated epithelial cells); (**B**) estrus (predominantly anucleated cornified cells); (**C**) metestrus (all three types of cells); and (**D**) diestrus 2 (majority of leukocytes). Scale bar = 100 µm. Magnification = 20x. Please click here to view a larger version of this figure.

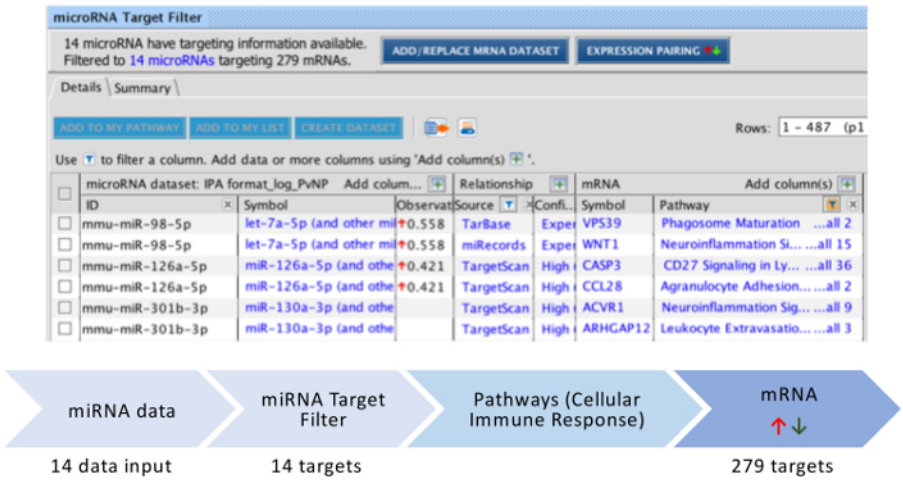

Figure 2: Functional analysis software representative results: miRNA target filter. Comprehensive profile of miRNAs at different stages of the estrous cycle. After performing miRNA filter, the software delivers detailed listings of genes and compounds implicated in diseases and other phenotypes, which can be filter and sort to get to certain pathways, in this case "Cellular Immune Response". Please click here to view a larger version of this figure.

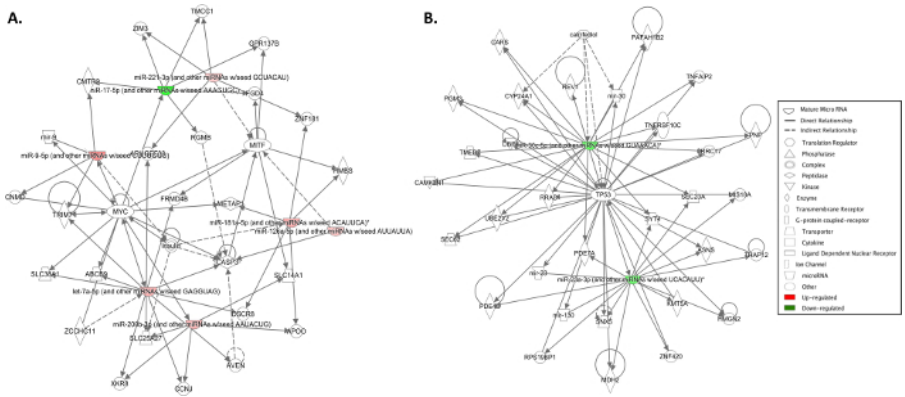

Figure 3: Functional analysis software representative results: networks. Comparison of networks affected by filtered air or ozone exposure in females at different stages of the estrous cycle. Diagram of biological networks associated with miRNAs in the lungs of female mice exposed to filtered air vs. ozone in proestrus (**A**) or non-proestrus stages (**B**). This figure has been modified from Fuentes et al.[6]. Please click here to view a larger version of this figure.

ID	Nucleic Acid (ng/µL)	A260/A280	A260/A230
Sample 1	1197.930	2.015	2.192
Sample 2	1355.703	2.018	2.223
Sample 3	2178.104	2.020	2.163
Sample 4	1600.837	2.010	2.139
Average	1583.144 ± 215	2.016 ± 0.002	2.179 ± 0.018

Table 1: Example of RNA concentrations and absorbance ratios at 260, 230, and 280 nm from purified lung tissue samples from four mice. Concentrations were measured with a spectrophotometer.

	logFC	t	P.Value	adj.P.Val	B
mmu-miR-694	1.492	4.071	0.000153	0.009514	0.759
mmu-miR-9-5p	0.836	3.916	0.000254	0.009514	0.289
mmu-miR-221-3p	0.385	3.106	0.003014	0.075361	-1.982
mmu-miR-181d-5p	0.597	2.891	0.005516	0.103424	-2.526
mmu-miR-98-5p	0.558	2.699	0.009243	0.138649	-2.987
mmu-miR-712-5p	0.667	2.563	0.013169	0.164609	-3.299
mmu-miR-106a-5p	-0.528	-2.412	0.019278	0.206547	-3.632

Table 2: *Limma* analysis results for differentially expressed miRNAs in females exposed to ozone *vs*. filtered air in the proestrus stage.

miRNAs ID	Observation 1	Observation 1	Observation 2	Observation 2
	Expr Log Ratio	**P Value**	**Expr Log Ratio**	**P Value**
mmu-miR-694	1.492	0.000153	0.543319208	0.0021385
mmu-miR-9-5p	0.836	0.000254	0.677595421	0.004997439
mmu-miR-221-3p	0.385	0.003014		
mmu-miR-181d-5p	0.597	0.005516	0.342276659	0.106467657
mmu-miR-98-5p	0.558	0.009243	0.455392799	0.034724699
mmu-miR-712-5p	0.667	0.013169		
mmu-miR-106a-5p	-0.528	0.019278		

Table 3: Example format for multi-observation upload of datasets to functional analysis software. Multiple experimental differential expressions can be grouped into a single spreadsheet and uploaded, and as many observations as needed can be added. Columns: 1) miRNAs ID; 2) Observation 1: Expr Log Ratio; 3) Observation 1: P Value; 4) Observation 2: Expr Log Ratio; 5) Observation 2: P Value.

Non-proestrus			**Proestrus**		
A. Genes targeted by differentially expressed miRNAs					
CAMK2N1	PAFAH1B2	SEC23A	ABCB9	FGD4	SLC25A27
CARS	PDE4B	SNX5	APOO	FRMD4B	SLC38A1
CYP24A1	PDE7A	SYT4	ARHGEF38	GPR137B	TMCC1
DBF4	PGM3	THAP12	AVEN	HMBS	TRIM71
HMGN2	PNP	TMED7	CASP3	METAP1	XKR8
KMT5A	REV1	TNFAIP2	CCNJ	MITF	ZCCHC11
LRRC17	RPS19BP1	TNFRSF10C	CMTR2	MYC	ZIM3
MDH2	RRAD	TP53	CNMD	RGMB	ZNF181
MIS18A	SEC62	UBE2V2	DSCR8	SLC14A1	
		ZNF420			
B. Differences in top diseases and biofunctions					
Diseases and Disorders		*P* Value	Diseases and Disorders		*P* Value
Inflammatory disease		3.84E-02 - 3.84E-05	Organismal injury and abnormalities		4.96E-02 - 2.77E-14
Inflammatory response		3.84E-02 - 3.84E-05	Reproductive system disease		2.15E-02 - 2.77E-14
Organismal injury and abnormalities		4.17E-02 - 4.17E-05	Cancer		4.96E-02 - 1.27E-10
C. Top molecular and cellular functions					
Molecular and Cellular Functions		*P* Value	Molecular and Cellular Functions		*P* Value
Cellular development		2.05E-02 - 5.26E-07	Cellular movement		3.77E-02 - 4.47E-07
Cellular compromise		3.75E-04 - 3.75E-04	Cellular death and survival		4.91E-02 - 5.61E-06
Cell cycle		2.62E-03 - 2.62E-03	Cellular development		4.97E-02 - 1.38E-06
D. Top physiological system development and function					
Development and Function		*P* Value	Development and Function		*P* Value
Organismal development		4.17E-02 - 1.31E-03	Embryonic development		3.30E-02 - 2.12E-05
Embryonic development		1.29E-02 - 1.29E-02	Connective tissue development and function		1.79E-02 - 6.10E-05
Connective tissue development and function		1.93E-02 - 1.93E-02	Tissue morphology		7.88E-05 - 7.88E-05
E. Top associated network functions					
Associated Network Functions		Score	Associated Network Functions		Score
Cellular development, inflammatory disease, inflammatory response		6	Organismal injury and abnormalities, reproductive system disease, cancer		19

Table 4: Functional analysis software summary of females exposed to ozone in the non-proestrus vs. proestrus stages. The functional analysis software allows the analysis of top canonical pathways, upstream regulators, diseases & functions, top functions, regulator effect networks and more. This table has been modified from Fuentes et al.[6].

Discussion

MicroRNA profiling is an advantageous technique for both disease diagnosis and mechanistic research. In this manuscript, we defined a protocol to evaluate the expression of miRNAs that are predicted to regulate inflammatory genes in the lungs of female mice exposed to ozone in different estrous cycle stages. Methods for the determination of the estrous cycle, such as the visual detection method, have been described[16]. However, these rely on one-time measurements, and therefore are unreliable. To accurately identify all estrous cycle stages in females that cycle regularly, the method described here is recommended. In addition, this simple protocol can also be used to indirectly estimate daily hormonal fluctuations in mice. To avoid activation of unwanted inflammatory responses due to vaginal irritation, sampling needs to be performed just once daily. Because of variability in the cycle length and housing influences, it is important to perform the protocol for two to three complete cycles before using animals in an experiment considering the cycle stage.

For the successful extraction of RNA from lung tissue, an accurate procedure is critical. This protocol describes a one-day method to isolate RNA from lung tissue that yields high-quality RNA. Modifications to the manufacturer's protocol were required to efficiently extract RNA from lungs. We added an additional centrifugation step after addition of the wash buffer to remove as much buffer as possible. We also eluted RNA with 35 µL of DNase/RNase-free water, centrifuging the column for 1.5 min to ensure high concentration levels. Spectrofluorometer results confirmed the effectiveness of our RNA extraction protocol. The ratio of absorbance at 260 and 280 nm (A260/280 ratio) is frequently used to assess the purity of RNA preparations. The maximum absorbance for nucleic acids is 260 and 280 nm, respectively. It is accepted as "pure" for RNA if the ratio is about 2.0[17]. Likewise, for the A260/A230 contamination absorbance ratio, the values for purity are in the range of 2.0–2.2[18].

In this study, the average A260/A280 and A260/A230 ratios observed were 2.016 ± 0.002 and 2.179 ± 0.018, respectively (**Table 1**). Therefore, our RNA extraction protocol was successful. Another advantage of the protocol used is the addition of the DNAse treatment. This is important to avoid genomic-DNA contamination[19]. A limitation of this RNA isolation protocol is the use of purification columns to discard waste through precipitation using alcohol because some lung debris may obstruct the membrane either partially or completely, resulting in low yields. Also, if the homogenization step is not carefully performed, large quantities of lung RNA can be easily lost or degraded. If low RNA yields are obtained, RNA can be re-purified and eluted in a smaller volume. Alternatively, RNA can be precipitated overnight following published protocols[20].

Microarray technologies applied to miRNA profiling are promising tools in many research fields. In our study, we used PCR arrays, which provide the advantage of higher detection threshold, and normalization strategies for detection of differentially expressed miRNAs vs. other technologies such as probe-based miRNA arrays[21]. A limitation of this protocol is that it requires a minimum amount of starting RNA material, and availability of specific sets of primers for the miRNAs of interest, as opposed to other available techniques such as RNAseq. Another advantage of PCR-based arrays is the option of using non-miRNA reference genes for qPCR normalization (such as small nucleolar RNAs or SNORDs) to calculate differential expression of miRNAs. Finally, using PCR arrays provides several options for data analysis, ranging from online tools provided by the manufacturers, to conventional methods to detect differential expression though Real-Time PCR. Statistical analysis with *limma* is convenient for both microarrays and PCR-based arrays and uses the empirical Bayes moderated *f*-statisitcs[22]. Here, we show that both p-values and q-values (adjusted for multiple testing) can be obtained with the command toptable adjusting the false discovery rate threshold and identifying differentially expressed miRNAs.

Functional analysis software is a web-based application for data analysis in pathway context. The software gives researchers powerful search abilities that can help to frame data sets or specific targets in context, within a bigger picture of biological significance. Although the software environment is flexible to different types of analysis (i.e., metabolomics, SNPs, proteomics, microRNA, toxicology, etc.), our goal here is to highlight aspects of miRNA analysis. After uploading a list of 14 miRNAs with significant expression log-ratios and p-values, all were mapped by the software. We performed the miRNA target filter and core analysis, which includes the enrichment pathway analysis. However, such analyses consider genes for which the 14 miRNAs are predicted to target and not the miRNAs themselves. The results section lists outputs such as: canonical pathways, diseases and function, genes targeted by differentially expressed miRNAs, physiological system development, regulators, and networks (**Table 4**). The pathway visualization is shown under the network tab, where miRNAs and molecules are shown as clickable nodes that are linked with information associated to the gene of interest (**Figure 3**). An advantage of the functional analysis software is the high-quality miRNA-related findings, including both experimentally validated and predicted interactions. The functional analysis software databases include: experimentally validated microRNA-mRNA interactions databases[23,24], predicted microRNA-mRNA interaction database with low-confidence interactions excluded (e.g., Target Scan)[25], experimentally validated human, rat, and mouse microRNA-mRNA interactions databases (e.g., miRecords)[26], and literature findings (e.g., microRNA-related findings manually curated from published literature by scientific experts). Other studies comparing the effectiveness and usability of bioinformatics tools to analyze pathways associated with miRNA expression confirm the effectiveness of this software[27]. Overall, computational methods are cost-effective, less time-consuming, and can be easily validated by molecular methods. With the constant growth and accumulation of biomedical data, bioinformatics methods will become increasingly powerful in the discovery of miRNA-mediated mechanisms of biological and disease processes.

Disclosures

The authors declare that they have no competing interests.

Acknowledgements

This research was supported by grants from NIH K01HL133520 (PS) and K12HD055882 (PS). The authors thank Dr. Joanna Floros for the assistance with ozone exposure experiments.

References

1. Rebane, A., Akdis, C. A. MicroRNAs: Essential players in the regulation of inflammation. *Journal of Allergy and Clinical Immunology.* **132** (1), 15-26 (2013).
2. Cannell, I. G., Kong, Y. W., Bushell, M. How do microRNAs regulate gene expression? *Biochemical Society Transactions.* **36** (Pt 6), 1224-1231 (2008).
3. Pritchard, C. C., Cheng, H. H., Tewari, M. MicroRNA profiling: approaches and considerations. *Nature Reviews Genetics.* **13** (5), 358-369 (2012).
4. Mi, S., Zhang, J., Zhang, W., Huang, R. S. Circulating microRNAs as biomarkers for inflammatory diseases. *Microrna.* **2** (1), 63-71 (2013).
5. Sessa, R., Hata, A. Role of microRNAs in lung development and pulmonary diseases. *Pulmonary Circulation.* **3** (2), 315-328 (2013).
6. Fuentes, N., Roy, A., Mishra, V., Cabello, N., Silveyra, P. Sex-specific microRNA expression networks in an acute mouse model of ozone-induced lung inflammation. *Biology of Sex Differences.* **9** (1), 18 (2018).
7. Aris, R. M., *et al.* Ozone-induced airway inflammation in human subjects as determined by airway lavage and biopsy. *American Review of Respiratory Disease.* **148** (5), 1363-1372 (1993).
8. Ritchie, M. E., *et al.* limma powers differential expression analyses for RNA-sequencing and microarray studies. *Nucleic Acids Research.* **43** (7), e47 (2015).
9. Krämer, A., Green, J., Pollard, J., Tugendreich, S. Causal analysis approaches in Ingenuity Pathway Analysis. *Bioinformatics.* **30** (4), 523-530 (2014).
10. Machholz, E., Mulder, G., Ruiz, C., Corning, B. F., Pritchett-Corning, K. R. Manual restraint and common compound administration routes in mice and rats. *Journal of Visualized Experiments.* (67), (2012).
11. Umstead, T. M., Phelps, D. S., Wang, G., Floros, J., Tarkington, B. K. In vitro exposure of proteins to ozone. *Toxicology Mechanisms and Methods.* **12** (1), 1-16 (2002).

12. Livak, K. J., Schmittgen, T. D. Analysis of relative gene expression data using real-time quantitative PCR and the 2(-Delta Delta C(T)) Method. *Methods.* **25** (4), 402-408 (2001).
13. Phipson, B., Lee, S., Majewski, I. J., Alexander, W. S., Smyth, G. K. Robust hyperparameter estimation protects against hypervariable genes and improves power to detect differential expression. *Annals of Applied Statistics.* **10** (2), 946-963 (2016).
14. Smyth, G. K., *et al.* Linear Models for Microarray and RNA-Seq Data User's Guide. *Bioconductor*. (2002).
15. Benjamini, Y., Hochberg, Y. Controlling the False Discovery Rate: A Practical and Powerful Approach to Multiple Testing. *Journal of the Royal Statistical Society. Series B (Methodological).* **57** (1), 289-300 (1995).
16. Byers, S. L., Wiles, M. V., Dunn, S. L., Taft, R. A. Mouse estrous cycle identification tool and images. *Public Library of Science ONE.* **7** (4), e35538 (2012).
17. Alves, M. G., *et al.* Comparison of RNA Extraction Methods for Molecular Analysis of Oral Cytology. *Acta Stomatologica Croatica.* **50** (2), 108-115 (2016).
18. Wilfinger, W. W., Mackey, K., Chomczynski, P. Effect of pH and ionic strength on the spectrophotometric assessment of nucleic acid purity. *Biotechniques.* **22** (3), 474-476, 478-481 (1997).
19. Bustin, S. A., *et al.* The MIQE guidelines: minimum information for publication of quantitative real-time PCR experiments. *Clinical Chemistry.* **55** (4), 611-622 (2009).
20. Walker, S. E., Lorsch, J. RNA purification- precipitation methods. *Methods in Enzymology.* **530,** 337-343 (2013).
21. Git, A., *et al.* Systematic comparison of microarray profiling, real-time PCR, and next-generation sequencing technologies for measuring differential microRNA expression. *RNA*. **16** (5), 991-1006 (2010).
22. Smyth, G.K. Limma: linear models for microarray data. *Bioinformatics and Computational Biology Solutions Using R and Bioconductor.* 397-420 (2005).
23. Griffiths-Jones, S. miRBase: the microRNA sequence database. *Methods Mol Biol.* **342**, 129-38 (2006).
24. Sethupathy, P., Corda, B., Hatzigeorgiou, A. TarBase: A comprehensive database of experimentally supported animal microRNA targets. *RNA*. **12** (2), 192-197 (2006).
25. Agarwal, V., Bell, G.W., Nam, J., Bartel, D.P. Predicting effective microRNA target sites in mammalian mRNAs. *eLife*. **4**, e05005 (2015).
26. Xiao, F., Zuo, Z., Cai, G., Kang, S., Gao, X., Li, T. miRecords: an integrated resource for microRNA-target interactions. *Nucleic Acids Res*. **37**, D105-D110 (2009).
27. Mullany, L. E., Wolff, R. K., Slattery, M. L. Effectiveness and Usability of Bioinformatics Tools to Analyze Pathways Associated with miRNA Expression. *Cancer Informatics.* **14,** 121-130 (2015).

